EFDA–JET–PR(07)61

Y. Andrew, N.C. Hawkes, T. Biewer, K. Crombe, D. Keeling, E. de la Luna,
C. Giroud, A. Korotkov, A. Meigs, A. Murari, I. Nunes, R. Sartori, T. Tala
and JET EFDA contributors

Evolution of the Radial Electric Field in a JET H-mode Plasma

Evolution of the Radial Electric Field in a JET H-mode Plasma

Y. Andrew[1], N.C. Hawkes[1], T. Biewer[2], K. Crombe[3], D. Keeling[1], E. de la Luna[4], C. Giroud[1], A. Korotkov[1], A. Meigs[1], A. Murari[5], I. Nunes[6], R. Sartori[7], T. Tala[8] and JET EFDA contributors*

JET-EFDA, Culham Science Centre, OX14 3DB, Abingdon, UK

[1]EURATOM-UKAEA Fusion Association, Culham Science Centre, OX14 3DB, Abingdon, OXON, UK
[2]Oak Ridge National Laboratory, Oak Ridge, TN 37831, USA
[3]Association EURATOM-Belgian State, Department of Applied Physics Ghent University, B-9000 Ghent, Belgium
[4]Asociasion EURATOM-CIEMAT para Fusion, CIEMAT, Madrid, Spain
[5]Consorzio RFX, ENEA-Euratom Association, Padua, Italy
[6]AssociaçãoEURATOM/IST,CentrodeFusãoNuclear,Lisbon, Portugal
[7]EFDA-CSU, Boltzmannstrasse 2, 85748 Garching, Germany
[8]Association EURATOM-Tekes, VTT, P.O. Box 1000, FIN-02044 VTT, Finland
** See annex of M.L. Watkins et al, "Overview of JET Results ",*
(Proc. 21 st IAEA Fusion Energy Conference, Chengdu, China (2006)).

Preprint of Paper to be submitted for publication in
Europhysics Letters

ABSTRACT.
Results are presented from recent measurements of the toroidal and poloidal rotation velocity in the pedestal region of an evolving JET H-mode plasma in which several transitions occur. These cover a range of plasma confinement regimes including L-mode, the L-H transition, ELM-free H-mode, ELMy H-mode and the H-L transition. Detailed edge plasma measurements show no spin-up of the poloidal rotation velocity prior to the L-H transition. However, directly following the transition to H-mode, the poloidal rotation velocity just inside the last closed flux surface increases to a maximum of 8(±2) km s^{-1}. As the H-mode continues to evolve, the largest values of edge toroidal and poloidal rotation velocity gradients are clearly associated with the ELM-free H-mode. Following the ELM-free phase, large, 1.4MJ ELMs are observed to erode the pedestal ion and electron temperature profiles along with the edge toroidal rotation gradient but have little impact on the overall poloidal rotation velocity shear. Maximum values of ±9 km s^{-1} are observed in the poloidal rotation velocity profile and have a significant effect on the temporal development of the edge plasma radial electric field.

1. INTRODUCTION

The H-mode is the current operation scenario envisaged for the next step magnetic fusion device, ITER [1]. Despite large progress in the development of the H-mode regime on tokamaks worldwide, anunderstanding of the triggering and sustainment mechanisms for the L-H transition, ELMy phases and the H-L transitions remains elusive. A great deal of the theoretical and experimental research has concentrated on the role of the radial electric field, E_r, at the L-H transition, for example see [1–5] and references therein. Large gradients in E_r in the edge plasma are thought to lead to shear in the **E×B** flow where transport due to plasma turbulence is substantially reduced at the formation of the transport barrier. Experimental studies have shown that gradients in E_r persist throughout H modes and are a general experimental feature of plasmas with an edge transport barrier. Results are presented in this paper from recent work to focus on this particular process, by considering the evolution of the plasma toroidal and poloidal rotation velocities and edge E_r over the changing phases of an H-mode plasma on JET.

Earlier experimental work in this area include very highly resolved measurements of Er at the plasma edge for a wide range of H-mode discharges on DIII-D [2]. A welllike structure was observed in E_r at the L-H transition in all plasmas. All the measured Er wells were negative with nearly the same spatial width, but differences in depth and under all conditions the shear in the Er profile persisted throughout the H-mode. The greatest contribution to E_r came from changes in impurity poloidal rotation velocity, v_θ, while the influence of the diamagnetic term only became appreciable tens of milliseconds into the H-mode as the ion pressure increased. The sign of carbon ion v was also observed to be consistently in the electron diamagnetic direction. More recent DIII-D measurements of v_θ profiles have been reported in [4] for Quiescent H-modes. Charge Exchange Recombination Spectroscopy (CXRS) on carbon and neon impurity species, was used to measure the E_r profile across the core and edge plasma. Following the application of velocity corrections

due to the energy dependent cross-sections, the experimental poloidal rotation profiles for both impurity species were found to be significantly greater than the neoclassical predictions. Recent enhancements to the JET edge plasma CXRS diagnostic have returned it to a balanced up-down symmetrical view of the neutral beam injection [6–8]. These changes together with new detectors allow accurate measurements of the v_ϕ, toroidal rotation velocity, v_r, ion temperature,T_i, and impurity density, n, profiles to be measured with fine spatial resolution across the pedestal region. This letter begins with a description of the experiment followed by the results from the CXRS measurements over an evolving H-mode plasma. The impact of the experimental data on the edge E_r profiles are also considered. The conclusions from this study are presented in the final section.

2. EXPERIMENT.

The evolution of the edge plasma rotation and Er is examined for Pulse No: 69937, a single null configuration with the ion ∇B drift towards the X-point, I_p/B_t = 2.5MA/2.7T and q_{95} = 3.3. This plasma had relatively high triangularity with δ = 0.36 and a divertor configuration such that the inner strikepoint remained on the inner vertical target, while the outer strikepoint location was on the outer horizontal target to accommodate the high lower triangularity. The various H-mode transitions were accessed by slowly ramping the neutral beam power up and then back down at a rate of 1 MW s^{-1}, as shown in figure 1. A constant level of 1MW of Ion Cyclotron Resonance Heating (ICRH) power was applied throughout the beam heating phase. The L-mode plasma ne was controlled using active gas feedback on the deuterium fuelling, also shown in figure 1, which led to variation of the level of gas puffing throughout the shot.

According to the force balance equation, Er can be written as:

$$E_r = \nabla P/neZ + v_\phi B_\theta - v_\theta B_\phi, \quad (1)$$

where P is the ion pressure, Z is the ion charge number, e is the electron charge, n is the ion density, v_ϕ and v_θ are the toroidal and poloidal velocities respectively and B_ϕ and B_θ are the toroidal and poloidal magnetic fields respectively. Equation () is valid for fuel and impurity ion species individually and in this paper all measurements were made with C^{6+} ions. It should be noted that the values and directions of v_ϕ and v_θ for different plasma ions can vary significantly from one another [2–5]. However, E_r and the E×B velocity shear, apply to all plasma species.

The edge plasma viewing CXRS system on JET has views along fourteen radial channels locations ranging from mid-plane radius of, R_{mid} = 3.65−3.85m (ρ ≅ 0.65−1.2) with spatial resolution ranging from 1.2 to 2.3cm and temporal resolution of 50ms. The balanced viewing geometry allows the measurements of v_ϕ and v_θ to be made self-consistently from line of sight velocities that have both toroidal and poloidal components. Further details on the diagnostic and its measurements can be found in [6].

The electron temperature, Te, has been measured witha multichannel Electron Cyclotron Emission (ECE) radiometer with a time resolution of 1ms. The electron temperature at the top of the pedestal

has been identified by the discontinuity in the gradient across the pedestal as defined in [9] and as used in previous JET studies [10–12]. The T_e at the pedestal top at the L-H transition is obtained by applying the pedestal position identified at the first clear H-mode T_e pedestal, to the T_e profile at the time of the transition. The line integrated edge n_e is measured with an interferometer along a single chord at R_{mid} = 3.74 m for this shot. The line average edge $\bar{n}_e$ has been calculated by dividing the measured line integrated ne by the chord length in the plasma.

3. RESULTS.

The L-H transition in this shot occurs at t = 17.7s and is characterised by the start of very small, irregular ELMs and increased values of plasma $\bar{n}_e$, stored magnetic energy, W_{dia} and confinement factor, H_{98}, indicated by the first vertical line in figures 1 and 2. The threshold power for access to the H-mode in this plasma was P_{th} = 6.8MW at an edge density of $\bar{n}_e = 1.8\times1019m^{-3}$. The confinement factor directly following the L-H transition, was H_{98} = 0.9 and it increased to 1.0 by the end of the first short, ELMy phase. The values of T_i, v_ϕ and v_θ at radial locations indicated in figure 3 by vertical, colour lines are plotted in their corresponding colours as a function of time in figure 2 and in more detail in figure 4 along with the divertor D signal. The radial profiles of the edge plasma T_i, T_e, v_ϕ, v_θ and E_r shown in figure 3 for time-slices in the L-mode phase, across the L-H transition and following the initial ELMy phase, all indicated by the corresponding vertical, colour lines in figure 4. During the L-mode phase (black and blue profiles) very little change is observed in the T_i and T_e profiles, with the pedestal top values of T_i = 790(±}22)eV and T_e = 320(±}32) eV for the last L-mode time-slice. A significant increase in the temperature pedestals can be seen in figures 3(a,b) and 4(b) following the transition to H-mode. The edge plasma v_θ profile remains close to zero throughout the L-mode phase as shown by the profiles in figure 3(d) and the corresponding time traces in figures 2(d) and 4(d). However, v_θ is observed to spinup along the outermost two channels (green profile) after the L-H transition, to a maximum value of 8 (±}2) km s^{-1} just within the Last Closed Flux Surface(LCFS). The edge v_ϕ profile also remains very flat at around 0 km s^{-1} during the L-mode phase as shown in figures 2(c), 3(c) and 4(c). At the start of the H-mode, however, the innermost channels measure a strong increase in v in the co-current direction (blue time traces), while just within the LCFS the plasma briefly spins up to 12 (±}5) km s^{-1} in the counter-current direction (black time-trace). Following the transition to the ELM-free phase all channels observe toroidal spin-up in the co-current direction and the development of a gradient in v_θ. The corresponding E_r profiles, figure 3(e), remain flat and close to 0 kV m^{-1} across the edge plasma in the L-mode phase. A gradient in E_r subsequently develops in the H-mode with a minimum value of –20 kV m^{-1} at the LCFS, green profile in figure 3(d) at t = 17.925s, with the v_ϕ component providing 65% of the value of the minimum in E_r.

On entering the ELM-free phase the plasma edge $\bar{n}_e$ continues to increase at a rate similar to that during the initial ELMy phase and the value of H_{98} increases from 1.0 to a maximum of 1.1 at 18.4s, as seen in figure 1. Both the T_e and T_i pedestals continue to develop during the ELM-free H-

mode, with the top of pedestals reaching maximum values of T_i = 1500 (±}15)eV and T_e = 870 (±}87)eV (blue profiles), shown in figures 5 and 6. The v_θ profile demonstrates a great deal of evolution during the ELM-free phase, with the development of a sheared region of rotation across the T_i pedestal, as shown in figure 5(c). Just within the LCFS, v_θ decreases to around 2 km s^{-1} as the T_i gradient region moves further in towards the core plasma, as shown by the green and red profiles in figures 5(d) and by the black time-trace in 6(d). Over the same time period the channels closest to the pedestal top measure a gradual increase in v to a maximum of 7.0(±}1) km s^{-1} in the electron diamagnetic direction, see figure 5(d) and red trace in figure 6(d). At the same time, the innermost channel shown, see green and blue time traces in figure 6(d), increases to a maximum of −6(±}2) km s^{-1} in the ion diamagnetic direction. As shown by the red profile in figure 5(d) the overall effect is the development of a well-like structure in the v_θ profile across the edge plasma. The v_ϕ profile continues to develop during the ELM-free phase with spin-up in the co-current direction. While the region close to LCFS demonstrates relatively little increase in v_ϕ, the inner channels measure an increase from −9.6(±}7) km s^{-1} to −88 (±}4)km s^{-1} at 9 cm from the LCFS, as seen in the red and blue profiles of figure 5. The outermost channels on the other hand measure a small increase of 29(±}3) km s^{-1} over this time, resulting in steepening of the edge v_ϕ gradient. The profiles of E_r over this phase become more positive as v_θ profile increases across the edge plasma. The result is a steeper E_r gradient in the edge region, with the pressure and v_θ terms provide similar contributions in the pedestal region.

The first of three very large ELMs occurs at t = 18.9s. The T_i, T_e, v_ϕ, v_θ and E_r profiles across the second ELM are plotted in figure 7 and the corresponding time-traces over all three ELMs are shown in figure 8, for the corresponding radial locations. The three large ELMs were characterised by decreases in stored diamagnetic energy 1.1MJ, 1.4MJ and 1.2MJ respectively. Comparing the T_i profiles prior to the second large ELM (black and red profiles) with that directly after (blue profile), a decrease in T_i is first observed within 4cm of the LCFS, while the inner region maintains pre-ELM values. In the subsequent time-slice 50ms later, the inner channels also measure a decrease in T_i (green profile) and the overall decrease in T_i is from 1373(±}28)eV at 20.075s to 908(±}13.2)eV at 20.175s at the pedestal top. As shown in figure 7(b) the pedestal T_e also falls from 860(±}86)eV to a minimum of 200(±}20)eV following the ELM. These large ELMs also have a significant effect on the v_ϕ rotation profile, shown in figure 7(c), with the region 4 cm inside the LCFS the first to demonstrate a decrease in v_ϕ by a maximum of 56 km s^{-1}, (blue profile). In the following time-slice (green profile) the remainder of the edge v_ϕ profile is also reduced with the mitigation of the edge v_ϕ gradient. Despite these large changes in the temperature and v_ϕ pedestal profiles, v_θ is largely unaffected by the ELMs. The most sensitive channels lie within the T_i gradient region and can be seen in figure 2(d) and 8(d) to drop by 5(±}0.5) kms^{-1} in v_θ over each large ELM. The corresponding profiles of E_r shown in figure 7(e), show a degradation of the pedestal E_r gradient following the ELM, compare the red with green profiles. The main source of the reduction in E_r is from the 40% decrease of the v_ϕ term in the pedestal region following the ELM.

The input power ramp down starts at 20.4s and the third large ELM is directly followed by a phase of high frequency small ELMs, as shown in figures 1, 2 and 10. The H-mode remains in this high frequency ELMy phase until the transition to L-mode at 25.5s. The power threshold for the H-L transition in this shot was P_{HL} = 5.4MW at an edge $n_e = 1.7\times1019m^{-3}$. The confinement factor at the start of the high frequency ELMs falls to a minimum of of H98 = 0.9 at 21.4s and subsequently recovers to a maximum value of H_{98} = 1.1 at 22.71s, as shown in figure 1. The confinement factor remains at this value until 23.62s after which it gradually falls reaching a value of H_{98} = 1 at the H-L transition. Comparing figures 7 (red profile) with 9 (black and green profiles) the effect of the decrease in power and the onset of high frequency ELMs is first seen in the outermost, edge plasma, closest to the LCFS as a clear reduction in T_i. As the input power decreases further, the ELM frequency increases further, the rest of the T_i pedestal is also modified, with the pedestal T_i falling from 1310(±}20)eV to 700(±}17)eV (blue profile), the T_i barrier width also shrinks from 3cm to 2cm. A similar change in T_e pedestal is observed with a drop in the pedestal T_i from 906(±}91)eV to 423(±}42)eV. The v_θ profiles demonstrate a general erosion of the well-like structure in the profile as the power ramps down, with a reduction of δv_θ to a minimum value of 8(±}3) km s^{-1} at 25.48s preceding the H-L transition. The loss of shear in v_θ 300ms before the H-L transition can also be clearly seen in the time-traces shown in figure 10. Finally, the edge v_θ evolves to a very flat profile at around 0 km s^{-1} by the end of the ELMy H-mode also shown in figures 9 and 10. The degradation of all three terms over the power ramp down contribute approximately equally to the reduction and flattening off of the E_r profile towards the end of the ELMy phase as shown by the profiles in figure 9(e).

CONCLUSIONS.

Highly spatially resolved measurements of the edge T_i, T_e, v_θ, v_ϕ and E_r have been made on a non-stationary JET H-mode plasma. No evidence of spin-up of v prior to the L-H transition has been observed, although a clear increase in v_θ is recorded following the transition to H-mode. This localised spin-up precedes the onset of an ELM-free phase in which further development of the T_i, T_e, v_ϕ and v_θ profile structure is clearly seen. The very large ELMs that follow the ELM-free phase have a significant impact on the T_i and v_ϕ profiles, eroding the pedestal gradients. Despite these large changes to the edge plasma, v_θ remains relatively unaffected by the ELMs, with the overall profile structure and region of sheared flow surviving the ELM crashes. Finally, the back transition to L-mode has been examined by ramping down the total input power and momentum leading to a phase of high frequency, small ELMs. The pedestal T_i, T_e, v_ϕ and v_θ all demonstrate a gradual relaxation of their gradients over this time. The H-L transition is preceded by the disappearance of any significant v_θ shear. This may be due to the narrowing of pedestal width, leaving a region v_θ shear too small to resolve with the current diagnostic spatial resolution. However, the data for this shot indicates that while significant spin-up and development of shear in v_θ arises as a consequence of the high confinement phase, it is not required to enter or maintain the H-mode.

ACKNOWLEDGEMENTS

This work was carried out within the framework of the EFDA and was partly funded by the UK EPSRC and by the European Communities under the contract of Association between EURATOM and UKAEA. The views and opinions expressed herein do not necessarily reflect those of the European Commission.

REFERENCES

[1]. Ikeda K., et al., Nuclear Fusion, **47** (No.6) June 2007.

[2]. Gohil P., Burrell K.H. and Carlstrom T.N., Nuclear Fusion, **38** (1) (1998) p.93-102.

[3]. Testa D., Garzotti L. and Giroud C., Nuclear Fusion, **46** (5) (May 2006) p.562-579.

[4]. Solomon W.M., Burrell K.H., Andre R., Baylor L.R., Budney R., Gohil P., Groebner R.J., Hol- comb C.T., Houllberg W.A. and Wade M.R., Physics of Plasmas, **13** (056116) 2006.

[5]. Kim J. et al., Phys. Rev. Lett., **72** (1994) 2199.

[6]. Andrew Y., Hawkes N.C. and Crombe K., Review Scientific Instruments, **77** (2006) 10E913.

[7]. Hawkes N.C. and Peacock, N., Review of Scientific Instruments, **63** (10) (1992) p.5164-p.5166.

[8]. Hawkes, N.C., Review of Scientific Instruments, **68** (5) (1997) p.2051-p.2059.

[9]. Breger P., Flewin C., Zastrow K.-D., Davies S.J., Hawkes N.C., Konig R.W.T., Pietrzyk Z.A., Porte L., Summers D.D.R. and Von Hellerman M.G., Plasma Physics and Controlled Fusion, **40** (1998) p.347-59.

[10]. Righi E. et al., Nuclear Fusion, **39** ((1999)) p.309-319.

[11]. Andrew Y., Hawkes N.C., O'Mullane M.G., Sartori R., Beurskens M.N.A., Coffey I., Joffrin E., Loarte A., McDonald D.C., Prentice R., Saibene G., Suttrop W. and Zastrow K.-D., Plasma Physics and Controlled Fusion, **46** (2004) p.337-47.

[12]. Andrew Y., Sartori R., Righi E., de la Luna E., Hacquin S., Howell D., Hawkes N.C., Horton L.D., Huber A., Korotkov A. and O'Mullane M.G., Plasma Physics and Controlled Fusion, **48** (2006) p.479-488.

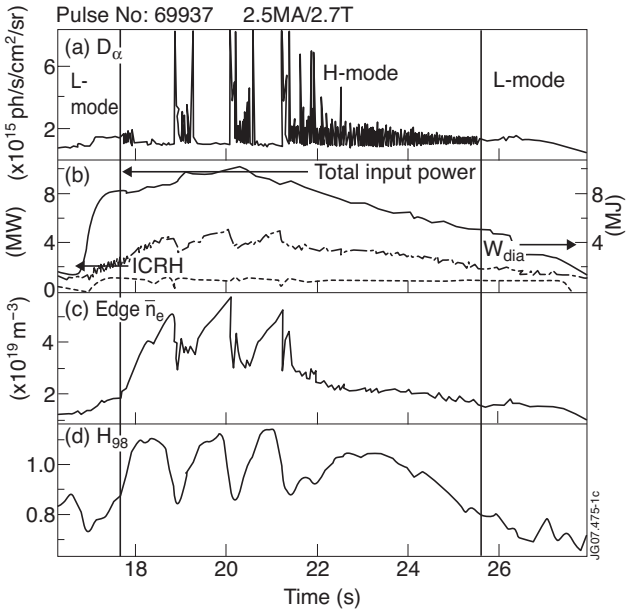

Figure 1: General plasma parameters for Pulse No: 69937. (a) Divertor D_α signal, (b) total input power, ICRH power and stored magnetic energy, (c) edge electron density, $\bar{n}_e$ and (d) H-mode confinement factor, H_{98}.

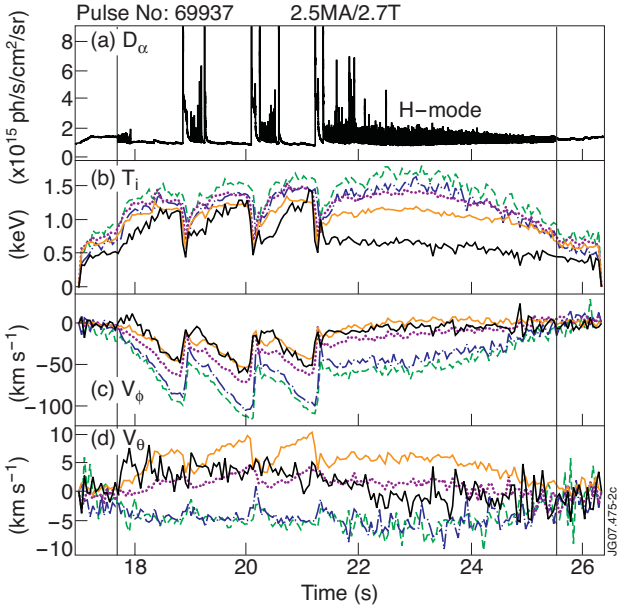

Figure 2: Overview of the T_i, v_ϕ and v_θ across the L-mode and H-mode phases of Pulse No: 69937 at I_p/B_t = 2.5MA/2.7T. The colour of each time trace corresponds to the radial location indicated in figure 3 by corresponding vertical lines of the same colour.

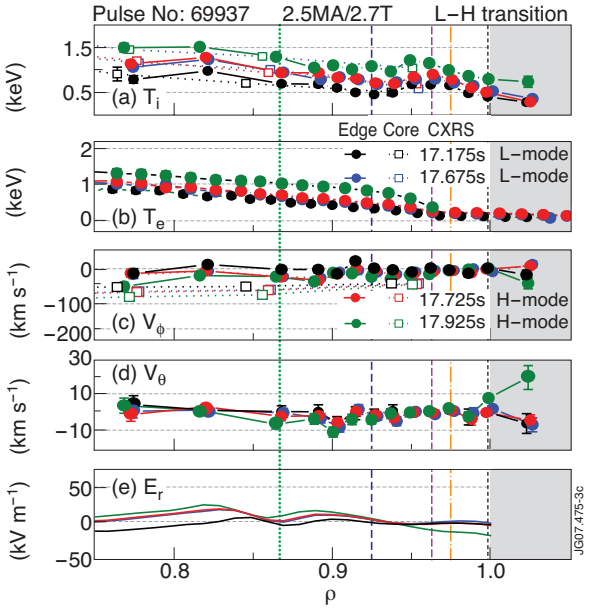

Figure 3: Radial profiles for the edge plasma (a) T_i, (b) T_e, (c) v_ϕ and (d) v_θ and (e) E_r values across the L-H transition for Pulse No: 69937. The vertical colour lines indicate the radial locations of the time traces in corresponding colours in figures 2 and 4.

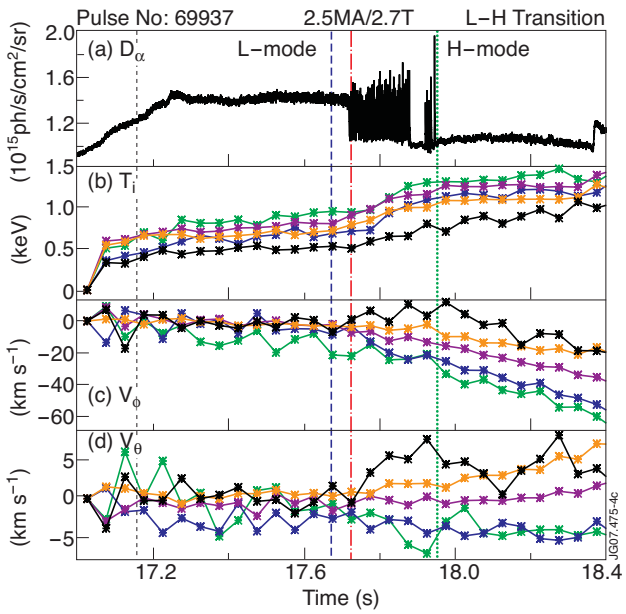

Figure 4: Time traces showing (a) the divertor D_α signal, (b) the edge T_i, (c) edge v_ϕ and (d) edge v_θ values for radial locations indicated in figure 3, across the L-H transition for Pulse No: 69937.

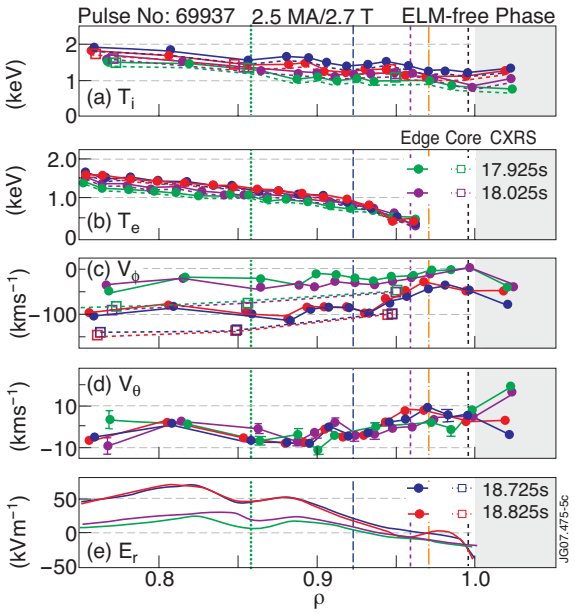

Figure 5: Radial profiles for the time-slices indicated by vertical lines in figure 6 in corresponding colours, in the ELM-free phase of the H-mode for Pulse No: 69937.

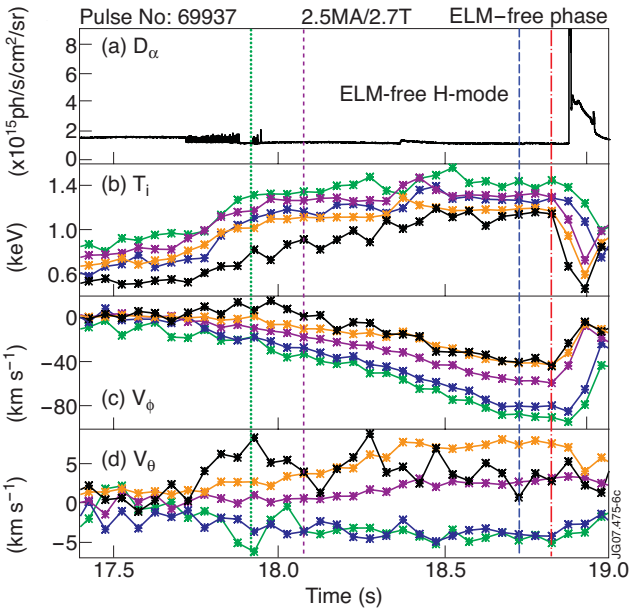

Figure 6: Time traces across the ELM-free phase of the H-mode for Pulse No: 69937 for (a) the divertor D_α, (b) edge T_i, (c) edge v_ϕ and (d) edge v_θ for corresponding radii indicated by vertical lines in figure 5.

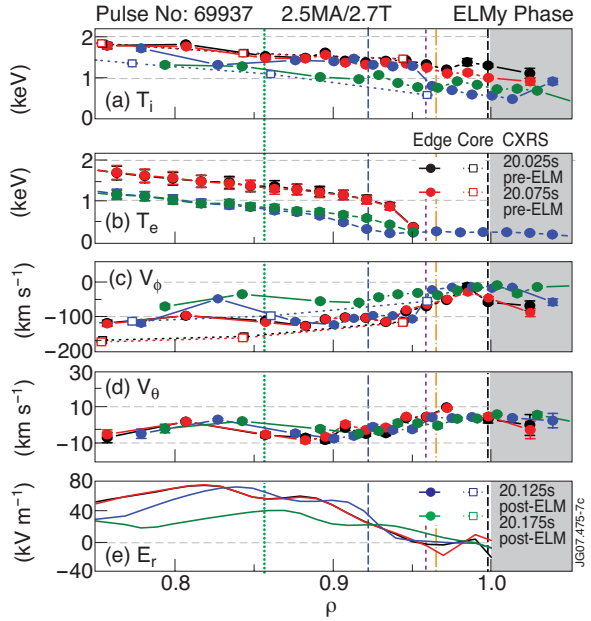

Figure 7: Radial profiles of (a) T_i, (b) T_e, (c) v_ϕ, (d) v_θ and (e) E_r before and following a large ELM indicated in figure 8, for Pulse No: 69937.

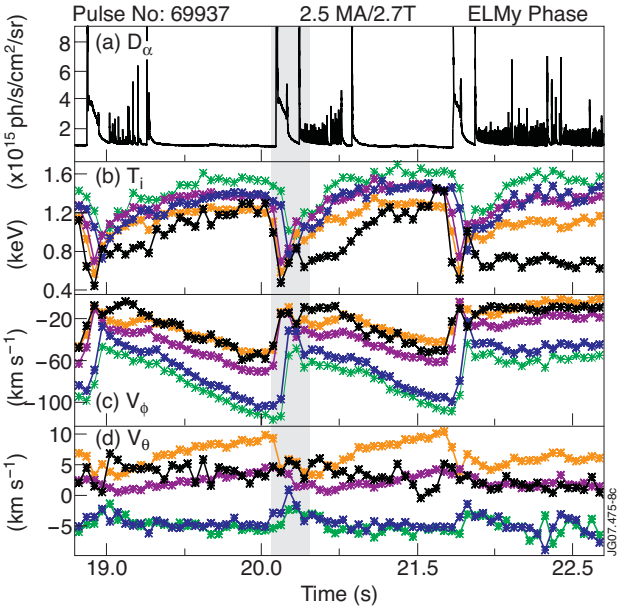

Figure 8: Time traces across the large ELMs phase of the H-mode for Pulse No: 69937.

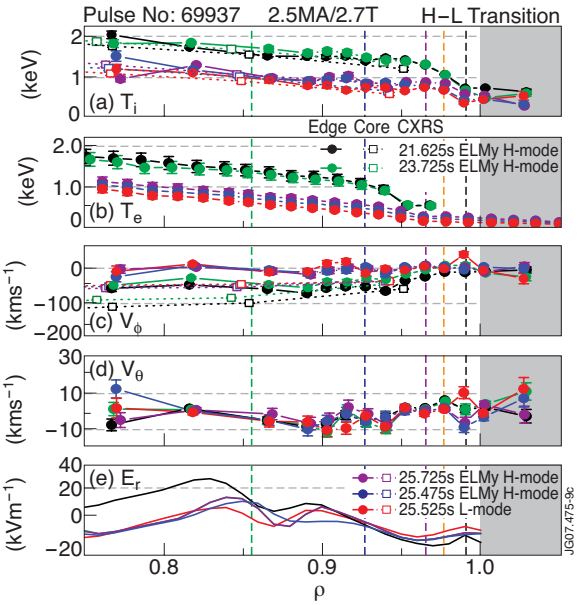

Figure 9: Radial profiles at the start of the high frequency ELM phase and across the H-L transition for Pulse No: 69937, for times indicated by vertical colour lines in figure 10.

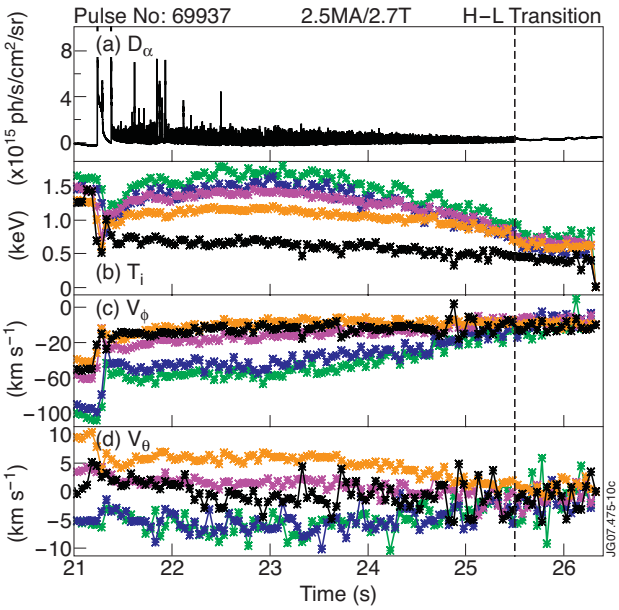

Figure 10: Time traces across the high frequency ELM phase and the H-L transition of Pulse No: 69937 for (a) the divertor D_α, (b)T_i, (c)v_ϕ and (d)v_θ, for radial channels indicated in figure 9 by vertical lines in corresponding colours.